Elastic electron scattering from the DNA bases cytosine and thymine

C. J. Colyer,[1] S. M. Bellm,[1] F. Blanco,[2] G. García,[3] and B. Lohmann[1]

[1]*ARC Centre of Excellence for Antimatter-Matter Studies, The University of Adelaide, Adelaide, South Australia 5005, Australia*

[2]*Departamento de Física Atómica Molecular y Nuclear, Facultad de Ciencias Físicas. Universidad Complutense, Avenida Complutense s/n, E-28040 Madrid, Spain*

[3]*Instituto de Física Fundamental, Consejo Superior de Investigaciones Científicas, Serrano 113-bis, E-28006 Madrid, Spain*

(Received 12 July 2011; published 14 October 2011)

Cross-section data for electron scattering from biologically relevant molecules are important for the modeling of energy deposition in living tissue. Relative elastic differential cross sections have been measured for cytosine and thymine using the crossed-beam method. These measurements have been performed for six discrete electron energies between 60 and 500 eV and for detection angles between 15° and 130°. Calculations have been performed via the screen-corrected additivity rule method and are in good agreement with the present experiment.

DOI: 10.1103/PhysRevA.84.042707 PACS number(s): 34.80.Bm

I. INTRODUCTION

The use of ionizing radiation in medicine is widespread. It is used commonly as a probe in radio-diagnostic examinations and as a therapeutic agent. Traditionally, the high-energy incident radiation was believed to cause the bulk of damage to biological tissue through ballistic impact. However, an appreciable amount of radiation damage (up to 50% [1]) is caused by secondary species that arise from the primary ionization [2]. After entering the biological medium, the primary ionizing particle deposits the majority of its energy via various scattering processes, such as excitation and ionization. This large energy transfer liberates large numbers of low-energy (0–20 eV) secondary electrons, which, then, can interact with several different biological molecules. Significant damage to the DNA double helix results from single- or double-strand breaks by the process of dissociative electron attachment [3,4]. This occurs either directly or via the formation of free radicals and tends to create localized areas of radiation damage due to the short thermalization distances of the low-energy secondary electrons.

Since radiation damage is caused by secondary particles as well as the primary particle, it is desirable to model their trajectories through a biological medium. This enables the nature, location, and intensity of cellular damage to be predicted and to be understood. Charged-particle track structures [5] map the path along which the primary and secondary species travel as they pass through the medium. These stochastic simulations incorporate the full spectrum of interactions of the primary and secondary particles at an individual atomic or molecular level via cross-section data. Due to the difficult nature of reliable measurement or calculation of cross-sectional data for electron scattering from large molecules, there is limited information on species of biological interest.

Experimental elastic differential cross sections (DCSs) for electron scattering from water have been known for some time [6] and are commonly used in track structure simulations. Only recently have measurements appeared concerning more complex biological molecules, such as formic acid [7], variations of the tetrahydrofuran ring [8,9], alanine [10], and pyrimidine [11]. Because of the experimental challenges associated with producing vapor targets of these molecules, theoretical calculations tend to precede experimental investigation. Elastic electron DCSs for the nucleobases of DNA were calculated separately by Możejko and Sanche [12] as well as Blanco and Garcia [13,14]. Both excitation functions (differential in energy) and angular distributions (differential in angle) have been produced for the four DNA bases plus uracil. Interestingly, both studies realized that the angular distribution at a given energy for a given nucleobase can be related to any of the others. This relation is simply via the ratio of their molecular weights or via the ratio of the number of electrons present in the target.

This paper represents the first experimental determination of elastic DCSs for electron scattering from two of the DNA bases, cytosine and thymine. Angular distributions were measured for six individual energies between 60 and 500 eV with the experimental arrangement limiting detection to angles between 15° and 130°. Theoretical cross sections calculated by the screen-correction additivity rule (SCAR) method are also presented for cytosine and thymine under the same conditions. Since the measured DCSs are relative, they are only attributed absolute values by normalization to the SCAR calculation to give the best visual fit. Comparison is also made with the existing theoretical results by Możejko and Sanche [12] and with the previous experimental study of Maljković *et al.* [11] on pyrimidine, given the mutual similarities in chemical structure (see Fig. 1).

II. EXPERIMENT

The present paper was conducted in a conventional $(e,2e)$ spectrometer, the operation of which was recorded in detail elsewhere [15]. Only the elements pertinent to the present investigation are described here. The elastic angular distributions are obtained using the crossed-beam method. A beam of electrons, sourced from a conventional electron gun, is crossed perpendicularly with the gas target. Outgoing electrons are energy selected via a hemispherical electron energy analyzer and finally are detected using a channel electron multiplier. The second detector in the $(e,2e)$ spectrometer was removed for the duration of the study. Since the apparatus's normal mode of operation is to measure coincident electron ionization, there is

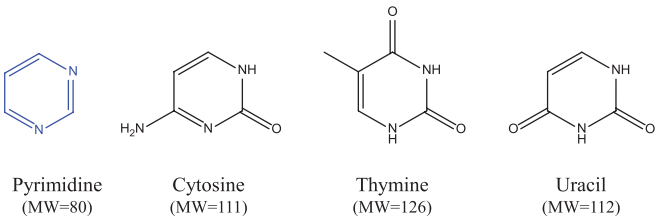

FIG. 1. (Color online) Chemical structures and molecular weights of the pyrimidine molecule and the pyrimidine nucleobases; cytosine, thymine, and uracil.

no provision in the experiment to establish absolute values for the cross sections.

A molecular-beam oven is used to heat the cytosine and thymine powder targets to produce a vapor. Manufactured from nonmagnetic 310 stainless steel, it is centrally housed in the spectrometer and is heated via two independent THERMOCOAX heating elements. The second independent element allows the outlet nozzle to be heated to a higher temperature to reduce clogging. Temperatures in excess of 300 °C have been achieved with good stability. As cytosine and thymine have different vapor pressures, the cytosine target was heated to a much higher temperature (220 °C) than thymine (145 °C) to achieve a reasonable level of signal. These temperatures are well below the thermal decomposition temperatures for both cytosine and thymine, and it is generally accepted that no thermal decomposition of cytosine occurs under vacuum for temperatures up to 220 °C [16].

It is essential to trap the target gases that are released from the molecular beam oven to prevent them from solidifying on the apparatus and vacuum chamber walls. The operation of the apparatus can significantly be affected by the deposition of the molecules on the electron optics. Mounted to the inside of the chamber lid, and concentric with the interaction region, a cold finger was installed. Made from 310 stainless steel, the cold finger had an oxygen-free high-conductivity copper collection disk at the end closest to the molecular oven. It was filled externally with liquid nitrogen by computer control and was proven to be quite effective in trapping the DNA bases.

III. CALCULATIONS

Cross sections for elastic scattering of 60–500 eV electrons by cytosine and thymine were calculated using a corrected form of the independent atom method (IAM) known as the SCAR procedure.

The first subjects of the present calculations are the atoms constituting DNA bases, namely, C, N, O, and H. We represent each atomic target by an interacting complex potential (i.e., the optical potential), whose real part accounts for the elastic scattering of the incident electrons while the imaginary part represents the inelastic processes, which are considered as absorption from the incident beam. To construct this complex potential for each atom, we followed the procedure of Staszewska *et al.* [17]. The real part of the potential is represented by the sum of three terms: (i) a static term derived from a Hartree-Fock calculation of the atomic charge distribution, (ii) an exchange term to account for the indistinguishability of the incident and target electrons, and (iii) a polarization term for the long-range interactions that depend on the target dipole polarizability. The imaginary part then treats inelastic scattering as electron-electron collisions. The actual imaginary potential used [18,19] included several corrections over the original one [17], such as the inclusion of screening effects or the description of the electron's indistinguishability [19]. This finally led to a model that provided a good approximation for electron-atom scattering over a broad energy range.

To calculate the cross sections for electron scattering from cytosine and thymine, we follow the IAM by applying a modified form of what is commonly known as the additivity rule (AR). In the AR approach, the molecular scattering amplitude is derived from the sum of all the relevant atomic amplitudes, including the phase coefficients, therefore, leading to the molecular DCSs for the molecule in question. Integral cross sections (ICSs) can then be determined by integrating those DCSs with the sum of the elastic ICS and the absorption ICS (for all inelastic processes except vibrations and rotations) then giving the total cross sections. Alternatively, ICSs also can be derived from the relevant atomic ICSs in conjunction with the optical theorem [19]. In its original form, we found an inherent contradiction between the ICSs derived from these two approaches, which suggested the optical theorem was being violated [11] by the first procedure. This problem was solved by employing a normalization procedure during the computation of the DCSs so that the ICSs derived from the two approaches were now entirely consistent [11]. Because no molecular structure is considered in the AR, it is only applicable when the incident electrons are fast enough that they effectively observe the target molecule as a sum of the individual atoms (typically well above 100 eV for the present sized molecules). To reduce this limitation, we introduced the SCAR method [14,20], which considered the geometry of the molecule (atomic positions and bond lengths) by employing some screening coefficients. With this correction, the range of validity might be extended to incident electron energies as low as 20 eV.

IV. RESULTS

Figure 2 shows DCSs for elastic scattering from cytosine at different incident electron energies of 500, 400, 300, 200, 100, and 60 eV. The measured cytosine cross sections are relative as the apparatus is not set up to allow the relative flow technique [21] to be employed. Absolute values are assigned to the measured data via normalization of the data set to the corresponding SCAR calculation to achieve the best visual fit. The uncertainties in the data displayed in the figure include only counting statistics and appear smaller than the data points. The statistical error in the data is less than 10% in most situations. Also included in the figure are calculations performed using the SCAR and IAM theoretical models and previous experimental data for pyrimidine [11].

The measured cross sections are very strongly forward peaked, which is attributed to the large dipole moments of both molecules. A small shoulder in the DCS is observed at angles between 40° and 60° in both the experimental data and the theoretical calculations. The exact location of this feature appears to be correlated with electron energy. At higher

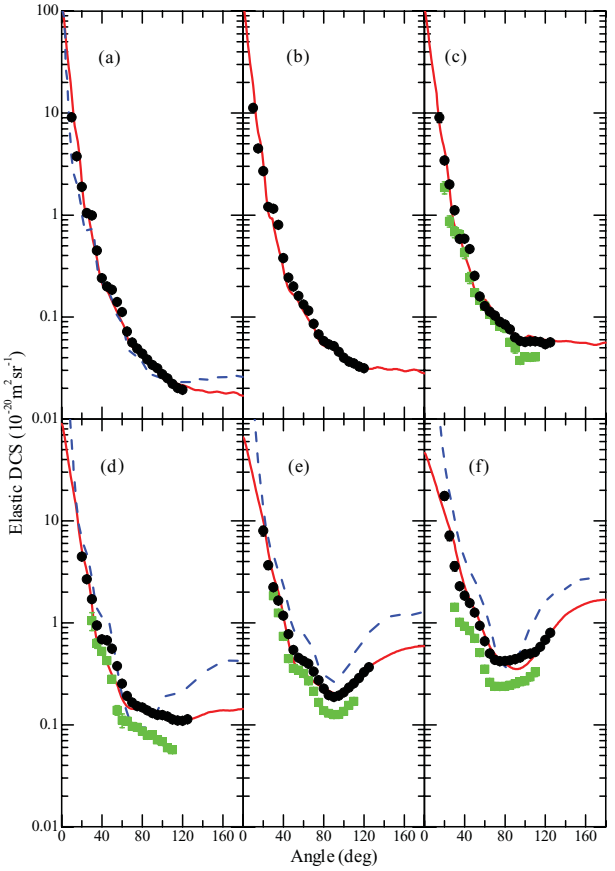

FIG. 2. (Color online) Relative DCSs for electron scattering from cytosine (circles) at energies of (a) 500 eV, (b) 400 eV, (c) 300 eV, (d) 200 eV, (e) 100 eV, and (f) 60 eV. The present data are attributed absolute values via normalization to the SCAR calculations at the corresponding energy (solid line). Also shown are the IAM calculations [12] (dashed line) and experimental data for pyrimidine [11] (squares) where available. The statistical error in the present experimental data is less than 10% in most cases.

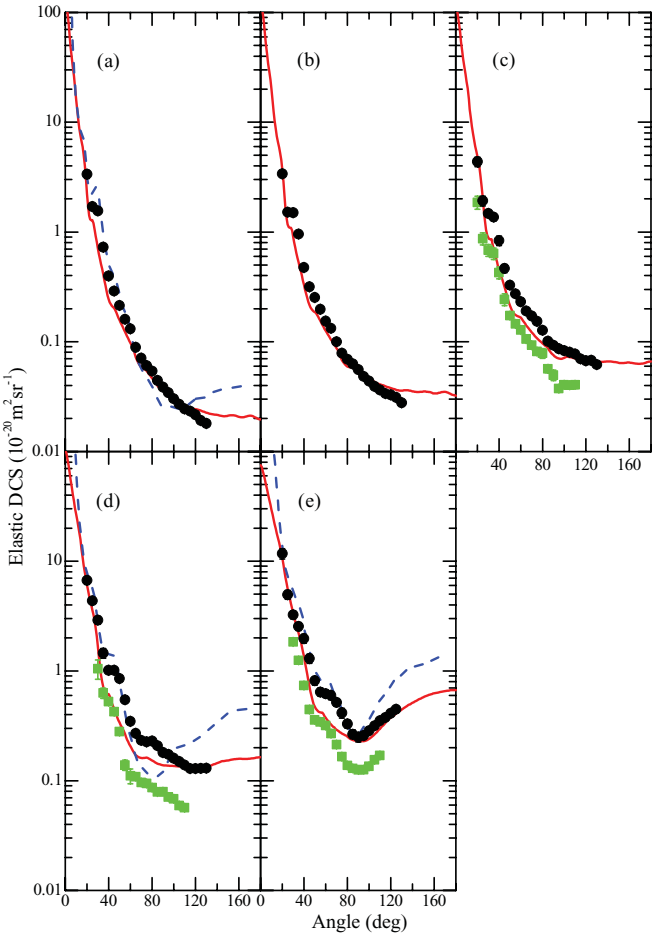

FIG. 3. (Color online) Relative DCSs for electron scattering from thymine (circles) at energies of (a) 500 eV, (b) 400 eV, (c) 300 eV, (d) 200 eV, and (e) 100 eV. Theory and pyrimidine experimental data as in Fig. 2. The thymine data are attributed absolute values via normalization to the SCAR calculations. The statistical error in the present experimental data is less than 10% in most cases.

incident electron energies, the shoulder shifts toward smaller scattering angles. There is an apparent lack of backward scattering in the measured cross sections for all but the two lowest-energy cases, i.e., 100 and 60 eV.

When comparison is made between the shape of the present cytosine data and the SCAR calculation, excellent agreement is observed between the calculated and the measured data sets, particularly with regard to the depth and location of the minima in the angular distributions. The SCAR calculation slightly underestimates the small shoulder in the cross section seen at approximately 40°. This is most noticeable at 200 and 100 eV [panels (d) and (e)]. The present data are also compared to the available IAM calculation of Możejko and Sanche [12]. Unfortunately, the IAM data are only available for four energies in our measured energy range, namely, 500, 200, 100, and 50 eV [panels (a) and (d)–(f), respectively], and the 50-eV calculation is compared to our measurements at 60 eV. Quite good agreement is seen with the IAM calculation; however, it tends to overestimate the size of the cross section at backward angles. In contrast to the SCAR method, the IAM results overestimate the size of the shoulder at around 40° at all available energies. A strong minimum in the 200-eV cross section is also predicted by the IAM, which is not observed in the present data. Finally, the measured cytosine distributions are compared to previous experimental data for pyrimidine of Maljković *et al.* [11] at 300, 200, 100, and 50 eV [panels (c)–(f)]. No internormalization is used to compare between the cytosine and the pyrimidine data, as the pyrimidine data are absolute, determined using the relative flow method. Clearly, the shape of the pyrimidine cross sections mimics the recently measured cytosine distributions quite well. The absolute magnitude of the calculated cytosine cross section is slightly greater than the pyrimidine cross section, most noticeably around the minimum of the DCSs. This can likely be attributed to the previously mentioned difference in molecular weight [13].

Relative DCSs for elastic electron scattering from thymine are presented in Fig. 3 for the same incident electron energies as cytosine, with the exception that the 60-eV measurement is not included. This is due to difficulty in obtaining a stable electron beam at this low energy with a thymine target. The DCSs for thymine appear very similar in shape to those for cytosine in Fig. 2. However, the magnitude of the small shoulder at around 40° appears larger for thymine than for cytosine.

The thymine data are compared with the results of the SCAR calculation, again with absolute values attributed to the experimental data via normalization to the theory. The SCAR calculation is once more very successful at reproducing the measured cross sections, although the shoulder that appears in the cross sections at 40° is still underestimated. This is most evident for the case of 200-eV incident electrons [panel (d)], where there also is an underestimation of the cross section near 80°.

As for cytosine, the thymine data are compared to the IAM calculation [12], similarly only available at 500, 200, and 100 eV [panels (a), (d), and (e)]. Quite good agreement is seen; however, many of the issues observed for cytosine occur again. The predicted cross sections are still overestimated at backward angles, and the deep minimum predicted by the IAM calculation at 200 eV does not manifest itself in the measured cross section. Nevertheless, the IAM results predict the shoulder in the cross sections near 40° much better in the case of thymine, particularly with regard to its magnitude. Indeed, there is very good reproduction of the experimental DCS for 100-eV incident electrons, with the exception of some overestimation of the cross section at larger angles.

The experimental thymine DCSs are compared to previous experimental cross sections for pyrimidine [11] for 300-, 200-, and 100-eV incident electrons [panels (c)–(e)]. While the shape of the thymine cross sections also matches the pyrimidine data quite well, the shoulder near 40° appears to be larger for thymine than for both cytosine and pyrimidine. The absolute magnitude of the thymine cross section, as assigned by the SCAR calculation, is greater than both the cytosine and the pyrimidine cross sections. Again, this is expected as a consequence of its greater molecular weight.

For both cytosine and thymine, the SCAR and IAM calculations differ more significantly from each other at lower incident energies and backward angles. This is discussed in greater detail in Blanco and García [13] and is largely due to the diminishing importance of including screening effects at higher incident electron energies. Unlike the IAM calculation, the SCAR calculation accounts for simultaneous interactions of the incident electron with multiple target atoms and includes geometrical screening corrections for each atom from the rest of the molecule through the SCAR. However, at larger electron incident energies, atomic cross sections are reported to become smaller, and thus, the necessary overlapping corrections become smaller.

V. CONCLUSIONS

Experimental and theoretical elastic differential cross sections have been investigated for electron scattering from cytosine and thymine. Relative elastic differential cross sections have been measured at energies ranging from 60 to 500 eV using the crossed-beam method. The experimental data have been compared with theoretical cross sections performed using the SCAR procedure. Very good agreement has been found between the experiment and the SCAR results, which, in addition, are used to attribute absolute scale to the experimental data. The data are also found to agree reasonably well with previous theoretical cross sections of Możejko and Sanche [12], and our measured cross sections exhibit a strong similarity in shape to the recent experimental cross-section measurements by Maljković *et al*. [11] on pyrimidine. The good agreement between the theory and the present experimental results provides strong support for the use of these theoretical models in track structure modeling, although absolute cross-section measurements would be needed in order to verify the magnitude of the calculated cross sections.

ACKNOWLEDGMENTS

The authors gratefully acknowledge the Australian Research Council's (ARC) Centre of Excellence Program for providing funding. C.J.C. would like to acknowledge scholarship support from the Australian Government. Partial support from the Spanish Ministry of Science and Innovation (Project No. FIS 2009-10245) and the European COST Programme (Actions No. CM0601 and No. MP1002) is also acknowledged.

[1] B. Boudaïffa, P. Cloutier, D. Hunting, M. A. Huels, and L. Sanche, Radiat. Res. **157**, 227 (2002).
[2] V. Cobut, Y. Frongillo, J. P. Patau, T. Goulet, M. J. Fraser, and J. P. Jay-Gerin, Radiat. Phys. Chem. **51**, 229 (1998).
[3] B. Boudaïffa, P. Cloutier, D. Hunting, M. A. Huels, and L. Sanche, Science **287**, 1658 (2000).
[4] F. Martin, P. D. Burrow, Z. Cai, P. Cloutier, D. Hunting, and L. Sanche, Phys. Rev. Lett. **93**, 068101 (2004).
[5] D. T. Goodhead, Int. J. Radiat. Biol. **65**, 7 (1994).
[6] M. T. D. N. Varella, M. H. F. Bettega, M. A. P. Lima, and L. G. Ferreira, J. Chem. Phys. **111**, 6396 (1999).
[7] V. Vizcaino, M. Jelisavcic, J. P. Sullivan, and S. J. Buckman, New J. Phys. **8**, 85 (2006).
[8] C. J. Colyer, V. Vizcaino, J. P. Sullivan, M. J. Brunger, and S. J. Buckman, New J. Phys. **9**, 41 (2007).
[9] V. Vizcaino, J. Roberts, J. P. Sullivan, M. J. Brunger, S. J. Buckman, C. Winstead, and V. McKoy, New J. Phys. **10**, 053002 (2008).
[10] B. P. Marinković, F. Blanco, D. Šević, V. Pejčev, G. García, D. M. Filipović, D. Pavlović, and N. J. Mason, Int. J. Mass Spectrom. **277**, 300 (2008).
[11] J. B. Maljković, A. R. Milosavljević, F. Blanco, D. Šević, G. García, and B. P. Marinković, Phys. Rev. A **79**, 052706 (2009).
[12] P. Możejko and L. Sanche, Radiat. Environ. Biophys. **42**, 201 (2003).
[13] F. Blanco and G. García, Phys. Lett. A **360**, 707 (2007).
[14] F. Blanco and G. García, J. Phys. B **42**, 145203 (2009).
[15] C. J. Colyer, S. M. Bellm, B. Lohmann, G. F. Hanne, O. Al-Hagan, D. H. Madison, and C. G. Ning, J. Chem. Phys. **133**, 124302 (2010).

[16] M. Bazin, M. Michaud, and L. Sanche, J. Chem. Phys. **133**, 155104 (2010).
[17] G. Staszewska, D. W. Schwenke, D. Thirumalai, and D. G. Truhlar, Phys. Rev. A **28**, 2740 (1983).
[18] F. Blanco and G. García, Phys. Lett. A **295**, 178 (2002).
[19] F. Blanco and G. García, Phys. Rev. A **67**, 022701 (2003).
[20] F. Blanco and G. García, Phys. Lett. A **330**, 230 (2004).
[21] J. C. Nickel, P. W. Zetner, G. Shen, and S. Trajmar, J. Phys. E: J. Sci. Instrum. **22**, 730 (1989).